PIERRE AUGER OBSERVATORY

Mass composition of ultra-high energy cosmic rays: results from the Pierre Auger Observatory and their astrophysical implications

Alexey Yushkov

Oddělení astročásticové fyziky
Fyzikální ústav AV ČR, v.v.i.

FZU

Cosmic accelerators

E_{lab} up to 10^7 times larger than at the LHC, flux ≈ 1 part/km^2/year at 10^{19} eV

Spectral features → composition (elemental spectra) → sources, propagation

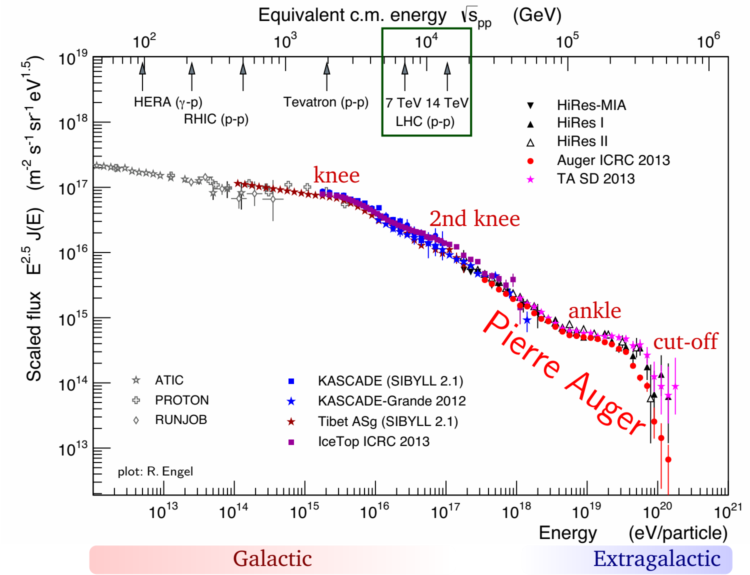

Galactic cosmic rays

Favored source candidate
[but there are alternatives]

Supernova remnants

$\downarrow$

Collisionless shock waves

$\downarrow$

Diffusive shock acceleration

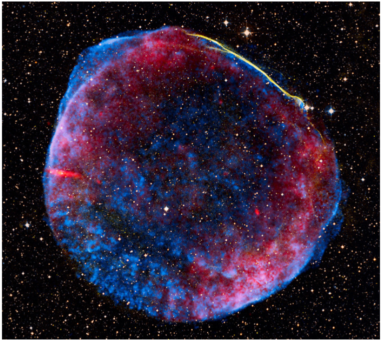

Injection and propagation scenarios: similar rigidity-dependent cut-offs

Injection: maximum source energy $E_{\rm max} \approx Z \times 3$ PeV

protons $E_{\rm max} \approx 3$ PeV, iron $E_{\rm max} \approx 80$ PeV

B. Peters, Il Nuov. Cim. 22 (1961) 800

Propagation: energy-dependent leakage from the Milky Way

knee-like structure in escape time at $E \approx Z \times \text{few} \times$ PeV

ratio of CR fluxes $\text{galactic/extragalactic} \approx 1/1$ at ≈ 200 PeV

Giacinti et al., PRD 90 (2014) 041302(R), 91 (2015) 083009

Extensive air showers (EAS)

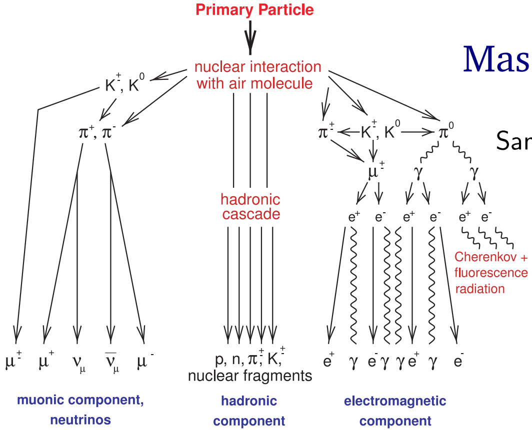

plot: A. Haungs et al., Rep. Prog. Phys., 66 (2003) 1145

Mass composition from EAS

↓

Sample particle distributions at ground

↓

Number of muons

$N_\mu \sim A^{1-\beta} \quad (\beta \simeq 0.9)$

↓

$$\frac{N_\mu(\text{iron})}{N_\mu(\text{proton})} \approx 1.4$$

proton $A = 1, \; \ln A = 0$

iron $A = 56, \ln A \approx 4$

KASCADE and KASCADE – Grande

KArlsruhe Shower Core and Array DEtector

KASCADE 200 × 200 m^2; KASCADE – Grande 700 × 700 m^2 scintillator arrays

2D electron – muon shower size spectra → primary spectra of 5 mass groups

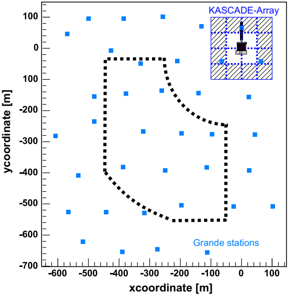

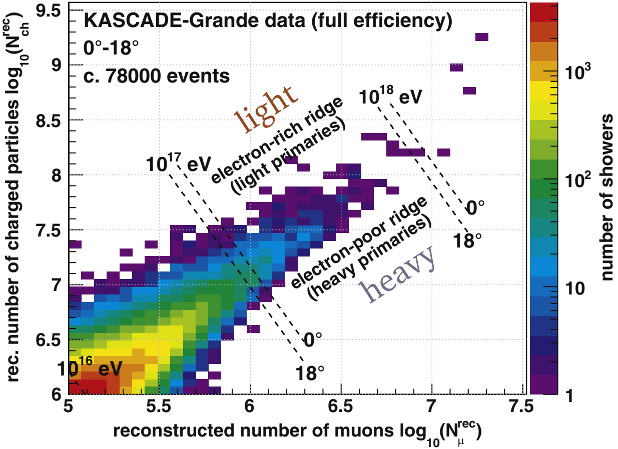

KASCADE – Grande, ApP 36 (2012) 183, 47 (2013) 54

KASCADE spectra in the knee region

Knee in light-element spectra at 3 – 5 PeV ($\Delta\gamma \approx 0.4$)

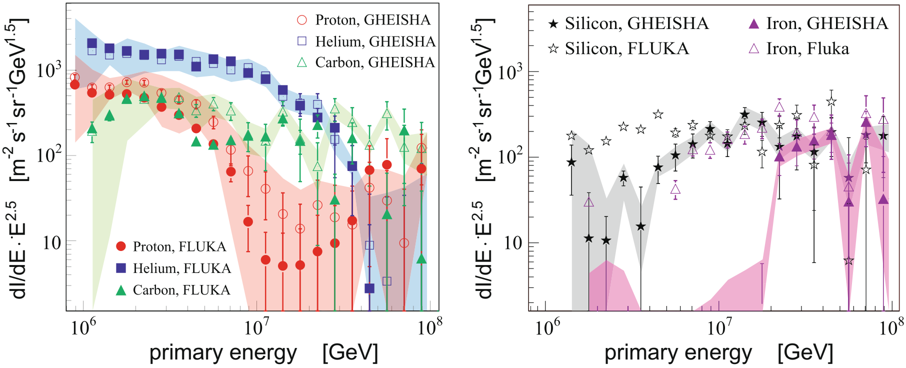

KASCADE, ApP 31 (2009) 86

KASCADE – Grande spectra in the 2nd knee region

Heavy component — knee at ≈ 80 PeV

Light component — hardening at ≈ 120 PeV

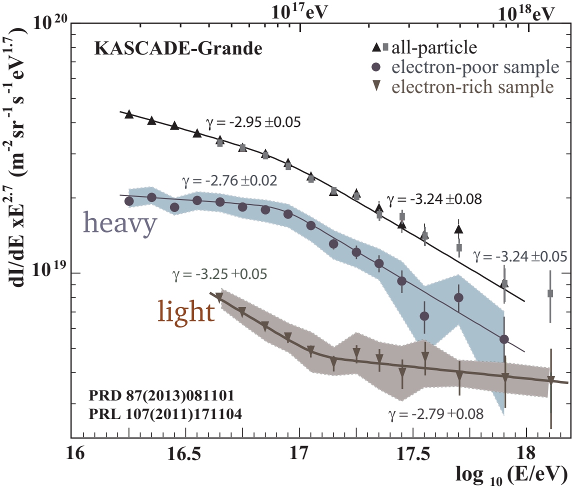

Start of transition to extragalactic component?

≈ 10 years ago: astrophysical models

'Ankle' and 'Mixed'

ankle — transition from galactic (≈ iron) to extragalactic CR (proton/mixed)

galactic ≈ extragalactic: $@E_{\rm ankle} \approx 5$ EeV ('Ankle'); $@E \approx 0.5 - 1$ EeV ('Mixed')

'Dip'

transition around 2nd knee (from ≈ iron to proton)

ankle — propagation effect due to $p + \gamma_{\rm CMB} \to p + e^+ + e^-$

cutoff — GZK effect $p + \gamma_{\rm CMB} \to p(n) + \pi^0(\pi^+)$

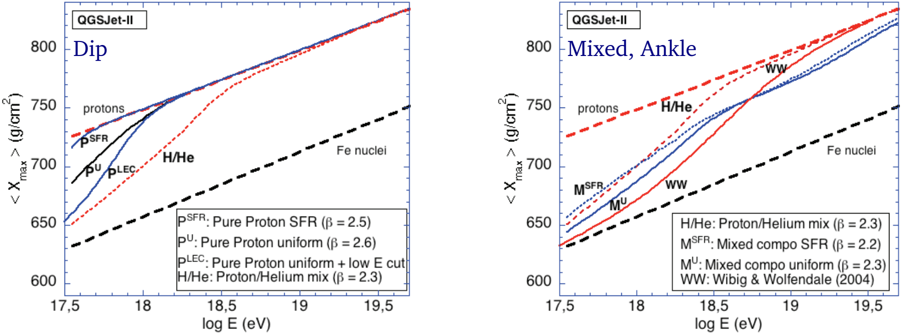

T. Wibig, A. Wolfendale, J. Phys. G 31 (2005) 255; A. Hillas, J. Phys. G 31 (2005) R95; V. Berezinsky et al., PLB 612 (2005) 147;
D. Allard et al. A&A 443 (2005) L29, A&A 473 (2007) 59; R. Aloisio et al., PRD 77 (2008) 025007

$\approx$ 15 years ago: data on mass composition $> 10^{17}$ eV

trend toward lighter composition, in agreement with astrophysical models?

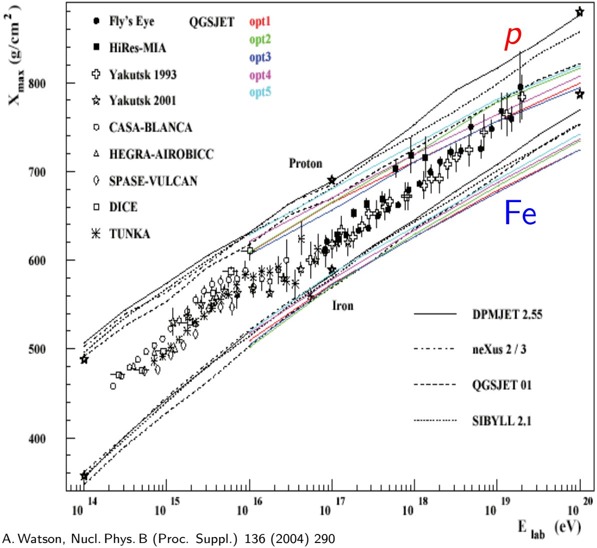

A. Watson, Nucl. Phys. B (Proc. Suppl.) 136 (2004) 290

$\approx$ 15 years ago: data on mass composition $> 10^{17}$ eV

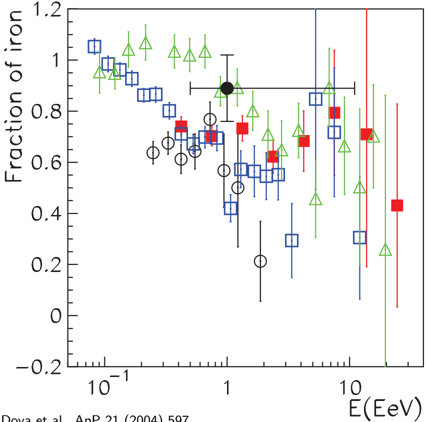

M.T. Dova et al., ApP 21 (2004) 597

Fig. 8. Fe fraction from various experiments: Fly's Eye (△), AGASA A100 (■), AGASA A1 (□) using SIBYLL1.5 ([6] and references therein) and Haverah Park [1], using QGSJET98 (○). The mass composition determined in this paper from Volcano Ranch data, using QGSJET98 (●), is shown, together with an estimate of the error and energy range.

"Our knowledge about the mass of primary CR at $E > 10^{17}$ eV is rudimentary"

A. Watson

The Pierre Auger Collaboration

$\approx$ 400 members from $\approx$ 90 institutions in 16 countries

The Pierre Auger Observatory

FD telescopes at Los Morados

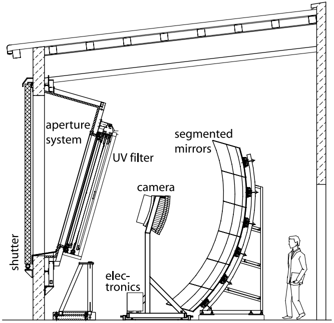

Water-Cherenkov station

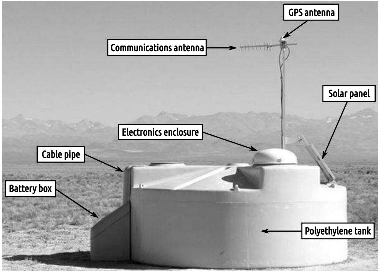

The Pierre Auger Observatory

FD telescopes at Los Morados

X_{max}, calorimetric energy

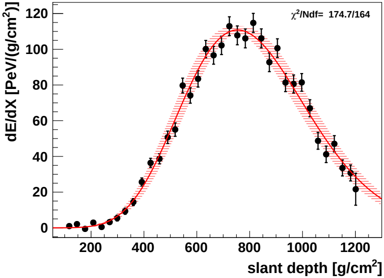

Water-Cherenkov station

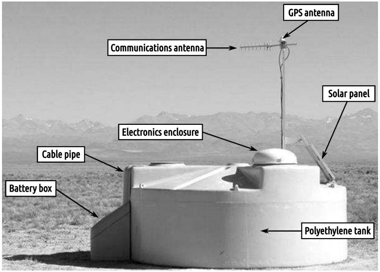

The Pierre Auger Observatory

FD telescopes at Los Morados

$X_{\max}$, calorimetric energy

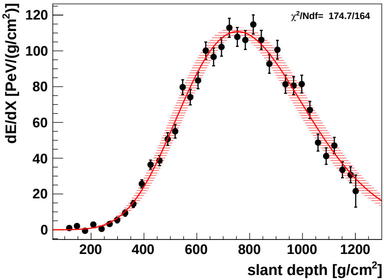

Water-Cherenkov station

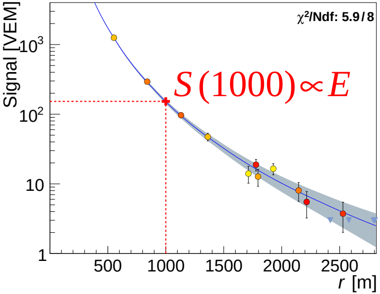

The Pierre Auger Observatory

Fluorescence detector (FD)

[longitudinal profile]

duty cycle 15 %

24 + 3 fluorescence telescopes at 4 locations

Surface detector (SD)

[lateral distribution]

duty cycle 100 %

1660 water-Cherenkov stations at 1500 m spacing, 3000 km^2

61 water-Cherenkov stations at 750 m spacing, 23.5 km^2

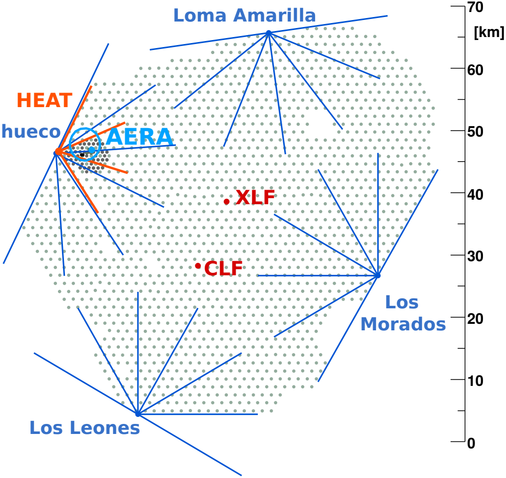

Mendoza province, Argentina

Nucl. Instrum. Meth. A798 (2015) 172

Longitudinal shower development

FD

$\approx$ calorimetric energy measurement

weak dependence on hadronic models

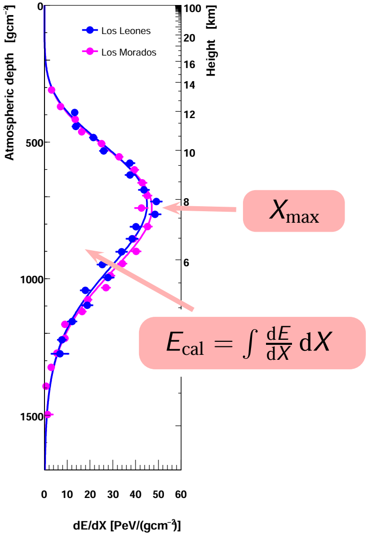

Mass composition sensitivity

$\langle X^{p}_{\max} \rangle \approx \langle X^{\mathrm{Fe}}_{\max} \rangle + (80 - 100)\ \mathrm{g\,cm^{-2}}$

$\sigma(X^{p}_{\max}) / \sigma(X^{\mathrm{Fe}}_{\max}) \approx 3$

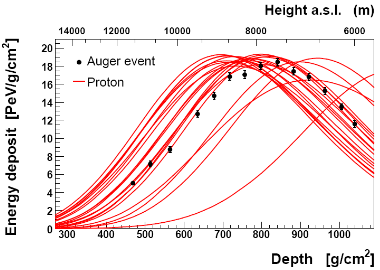

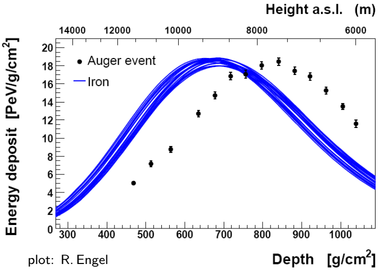

plot: R. Engel

Measurements of the depth of shower maximum X_{max}

11 years of data 12.2004 – 12.2015

energies $E > 10^{17.2}$ eV

the highest energy 107 ± 8 EeV

42662 high-quality FD events

842 events with $E > 10$ EeV

systematic uncertainty
below 10 $\mathrm{g\,cm^{-2}}$

resolution
26 $\mathrm{g\,cm^{-2}}$ at $10^{17.8}$ eV
15 $\mathrm{g\,cm^{-2}}$ for $E > 10^{19.3}$ eV

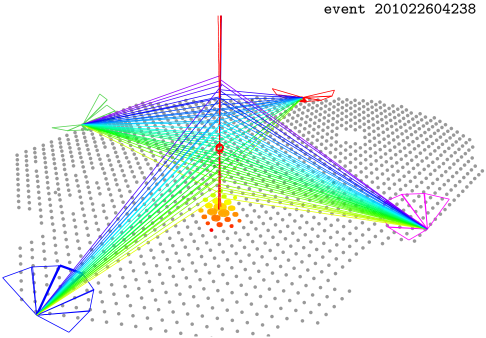

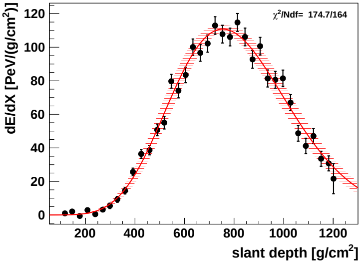

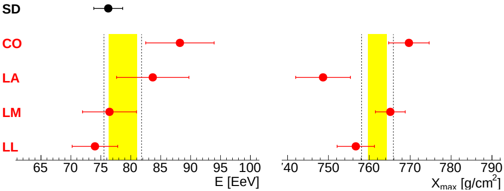

PRD 90 (2014) 122005, update at ICRC (2017)

Rate of change of X_{max} with energy

One of the most reliable mass indicators

simulations: $54 - 64$ [g cm^{-2}/decade] for constant composition

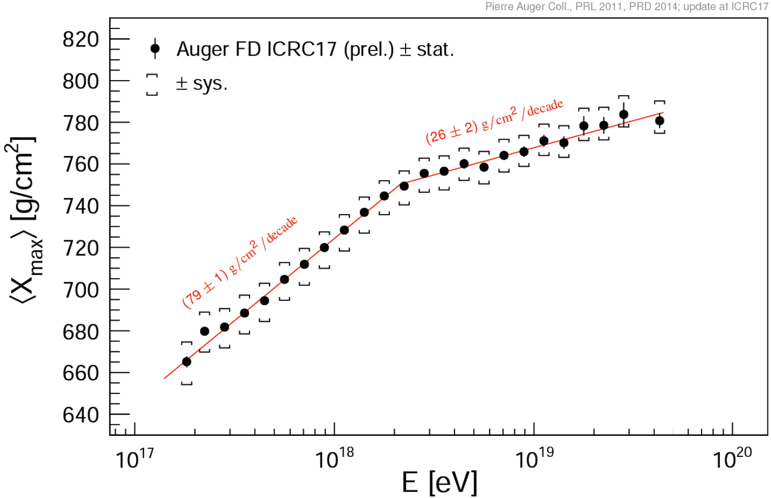

Composition is getting lighter below ≈ 2 EeV and heavier afterwards

$X_{\rm max}$ moments: data vs simulations

Composition is getting lighter below ≈ 2 EeV and heavier afterwards

PRD 90 (2014) 122005, update at ICRC (2017)

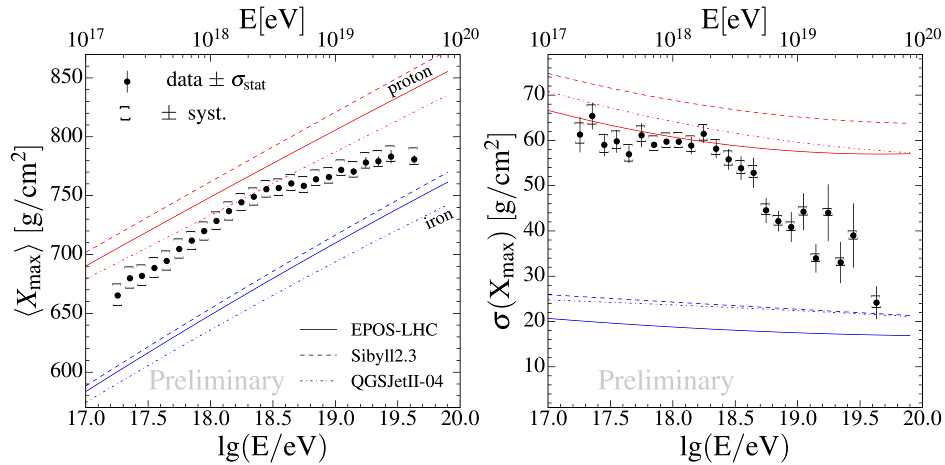

Composition from fits of X_{max} distributions

poor fit (p, Fe)

intermediate masses improve the fit quality (p, N, Fe) (p, He, N, Fe)

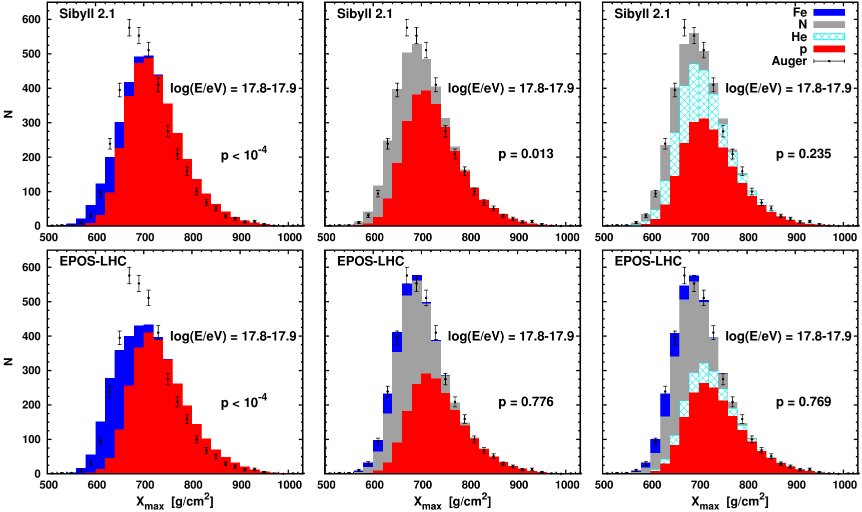

PRD 90 (2014) 122006, update at ICRC 2017

Auger: mass composition from fits of X_{max} distributions

fractions of p and He change much with energy, Fe is almost absent

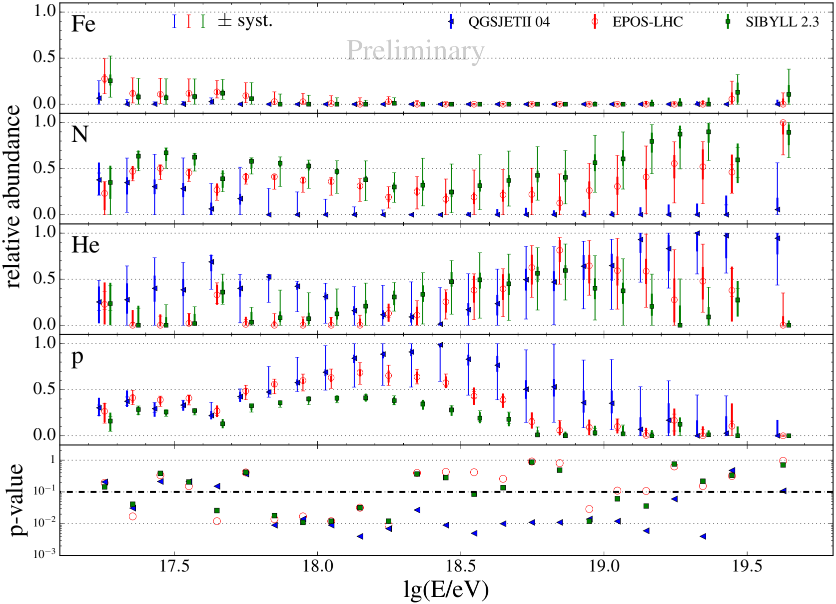

PRD 90 (2014) 122005, update at ICRC (2017)

'Ankle' in all-particle spectrum

one component changing slope? $\sigma(\ln A) \approx 0$ (as in 'dip' model)

several components with different slopes? $\sigma(\ln A) \neq 0$ (as in 'mixed' model)

...

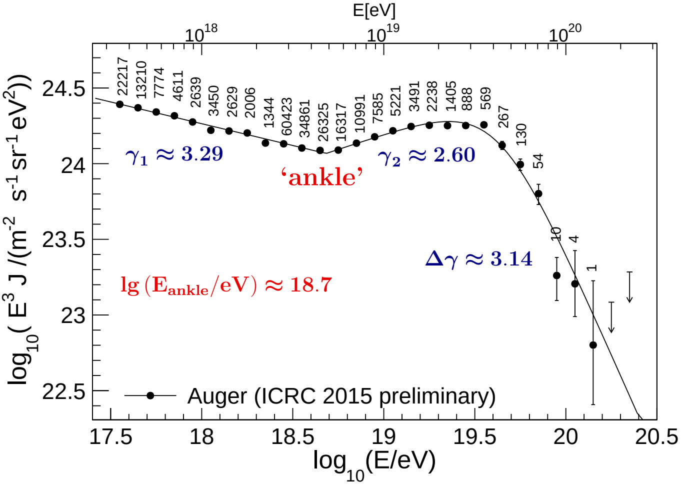

I. Valiño for Auger Collab., ICRC 2015, PoS 271

$\langle \ln A \rangle$ and $\sigma^2(\ln A)$ near 'ankle' ($\lg(E/\mathrm{eV}) \approx 18.7$)

conversion from first two moments of $X_{\max}$ distributions

[Auger, ICRC 2017]

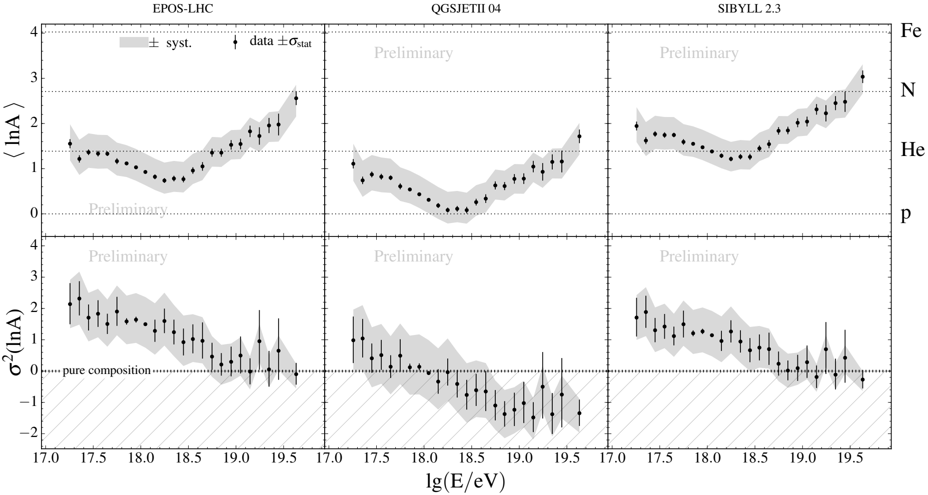

Less model-dependent estimate of $\sigma(\ln A)$?

Combine muon content N_μ and $X_{\max}$

properties follow already from the Heitler-Matthews model [J. Matthews, ApP 22 (2005) 387]

Depth of shower maximum

$$\langle X_{\max}\rangle = \langle X^p_{\max}\rangle - D_p \langle \ln A\rangle$$

$$\langle X^p_{\max}\rangle \approx \langle X^{\mathrm{Fe}}_{\max}\rangle + (80 - 100)\ \mathrm{g\,cm^{-2}}$$

arXiv:1604.03637

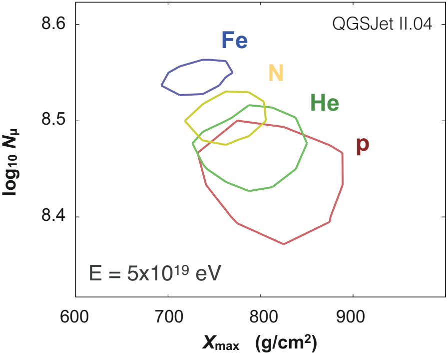

Number of muons

$N_\mu \sim E^\beta \ (\beta \approx 0.9)$

superposition model $1[A, E] \to A[1, E/A]$

$$N_\mu \sim A^{1-\beta}, \quad \frac{N_\mu(\mathrm{Fe})}{N_\mu(p)} \approx 1.4$$

Relative placement of nuclei in $(X_{\max}, N_\mu)$ is weakly model-dependent

The key idea

heavier nuclei produce shallower showers with larger signal (more muons)

general characteristics of air showers / minor model dependence

[P. Younk, M. Risse, ApP 35 (2012) 807]

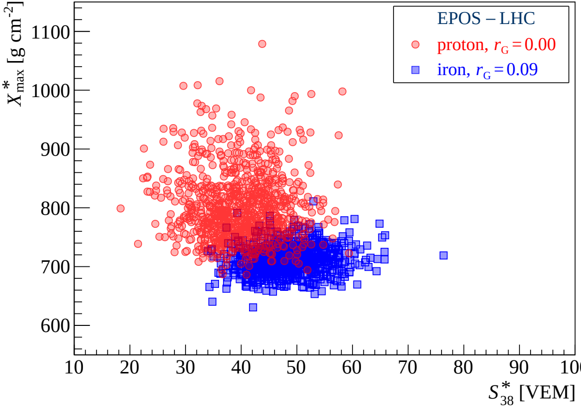

Correlation

EPOS-LHC

pure beams

0.00 for proton

$+0.09$ for iron

max mixing

-0.37 for $0.5\,p - 0.5\,\mathrm{Fe}$

More negative correlation ⇒ more mixed composition

S^*_{38}: SD signal at 1000 m from the core scaled to 10 EeV, 38°

X^*_{max}: X_{max} scaled to 10 EeV

[Auger, PLB 2016]

Data vs pure beams

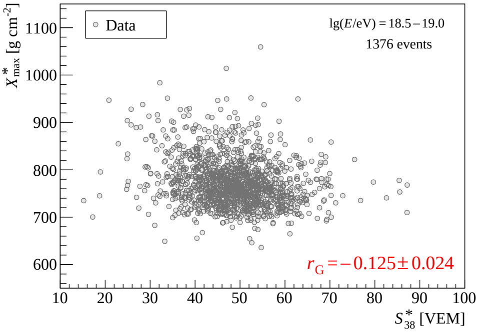

$r_G(X^*_{max}, S^*_{38})$ for protons

EPOS-LHC	QGSJetII-04	Sibyll 2.1
0.00	$+0.08$	$+0.07$

difference to data

$\approx 5\sigma$	$\approx 8\sigma$	$\approx 7.5\sigma$

difference is larger for other pure beams

difference is $\gtrsim 5\sigma$ for all p – He mixes

primary composition near the ankle is mixed

nuclei with $A > 4$ needed to explain data

systematics plays only a minor role $\sigma_{syst}(r_G) \lesssim 0.01$

due to invariance of r_G to additive and multiplicative scale transformations

r_G ranking correlation coefficient [R. Gideon, R. Hollister, JASA 82 (1987) 656]

$r_G(X^*_{max}, S^*_{38})$ vs dispersion of masses $\sigma(\ln A)$

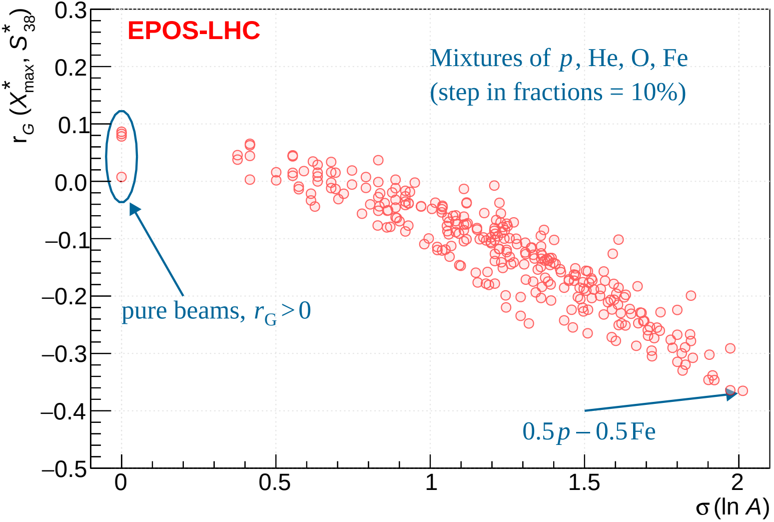

Dispersion of masses: data vs simulations

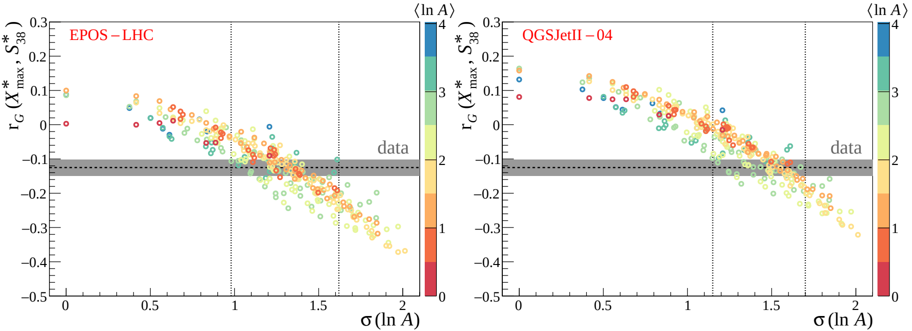

data are compatible with dispersion of masses $\sigma(\ln A) \simeq 1.35 \pm 0.35$

$X_{\max}$ from the SD up to 100 EeV

PRD 96, 122003 (2017)

Risetime $t_{1/2}$ — time of increase from 10% to 50% of total integrated signal

time traces of SD stations

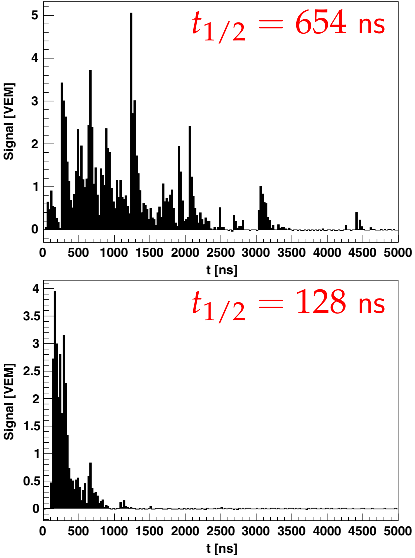

$t_{1/2}$ sensitivity to shower development stage

↓

mass of the primary particle

$t_{1/2}$ sensitivity to EM/μ

↓

hadronic interactions

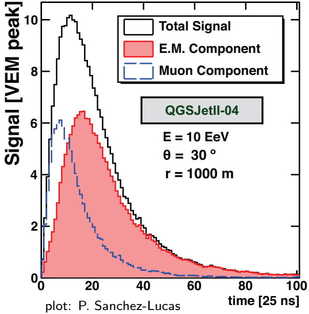

plot: P. Sanchez-Lucas

X_{max} from the SD up to 100 EeV

PRD 96, 122003 (2017)

Calibration with X_{max} from the fluorescence detector

events

750 m	1500 m
27553	54022

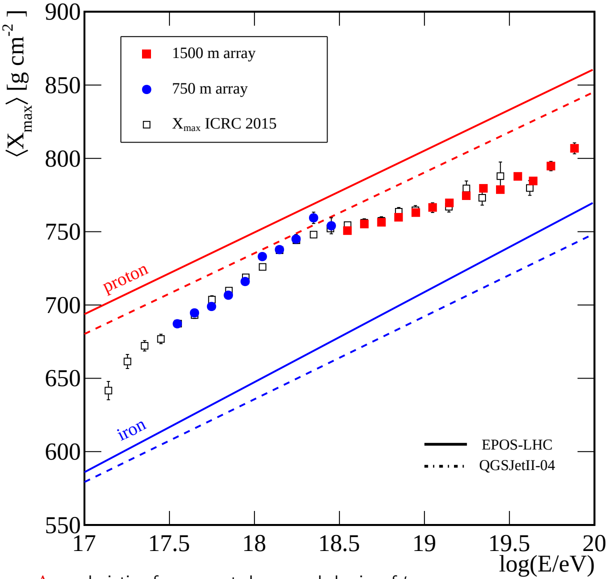

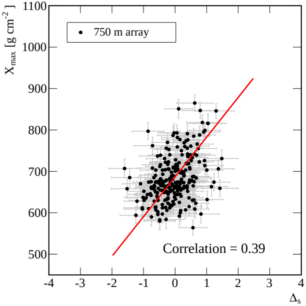

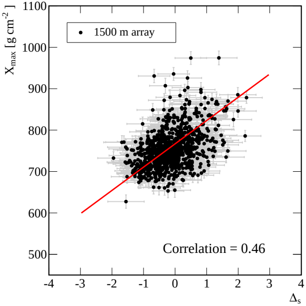

Δ_s — deviation from expected average behavior of $t_{1/2}$

$X_{\max}$ from the SD up to 100 EeV

PRD 96, 122003 (2017)

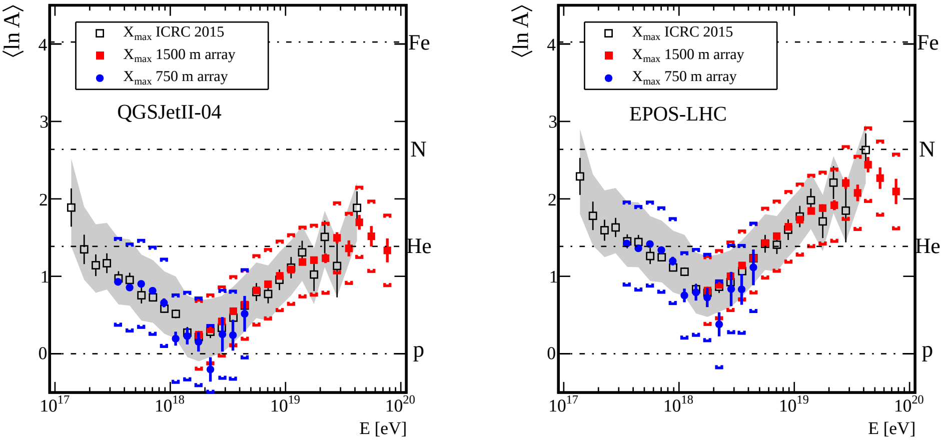

compatible results from FD $X_{\max}$ and Δ-method

first indications that rise of primary mass might be stopping above 50 EeV

Open questions

'Old' astrophysical models ('ankle', 'dip', 'mixed') are disfavored

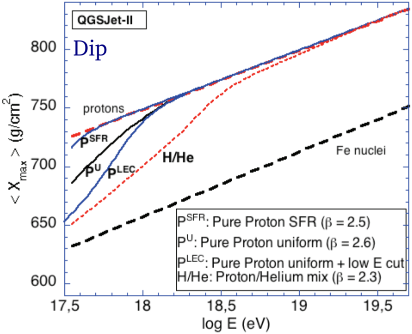

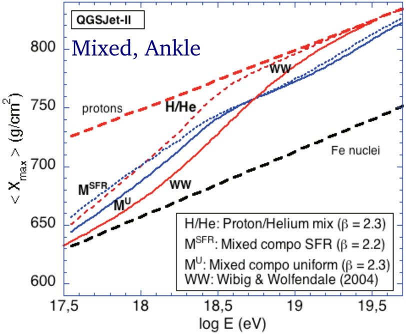

Is there a subdominant light component at the highest energies?

If not, can we discover sources for observed mixed/heavy composition?

End of the CR spectrum: nuclei fragmentation or maximum source energy?

How to describe energy spectrum and evolution of the mass composition?

Astrophysical model for spectrum–composition fit

JCAP 04 (2017) 038

sources: extragalactic, identical, uniformly distributed, no evolution

injected nuclei: ^{1}H, ^{4}He, ^{14}N, ^{28}Si, ^{56}Fe

cutoff: rigidity ($R = E/Z$) dependent

cosmic photon background: CMB, extragalactic background light

energy losses: $\mathrm{e}^{+} - \mathrm{e}^{-}$ and photo-meson production, photo-disintegration

extragalactic magnetic fields: no interaction (1D propagation)

propagation software: SimProp, CRPropa

energy range: $E > 5$ EeV (above 'ankle' feature of spectrum)

interactions in atmosphere: EPOS-LHC, QGSJetII-04, Sybill 2.1

data to fit: SD spectrum (47767 events), X_{max} distributions (1446 events)

Astrophysical model for spectrum–composition fit

JCAP 04 (2017) 038

composition at source

$f_{\mathrm{He}} = 67.3\%$, $f_{\mathrm{N}} = 28.1\%$, $f_{\mathrm{Si}} = 4.6\%$

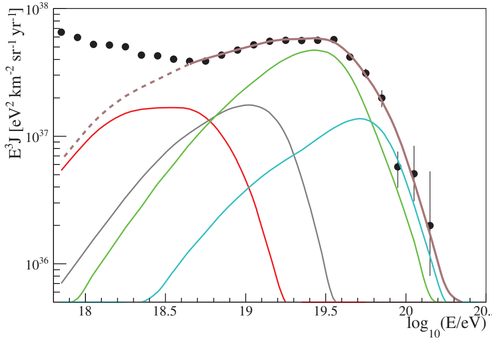

hard injection spectra $\gamma = 0.96^{+0.08}_{-0.13}$

low rigidity cutoff $\lg(R/\mathrm{V}) = 18.68^{+0.02}_{-0.04}$

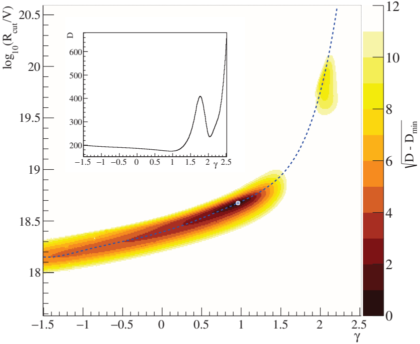

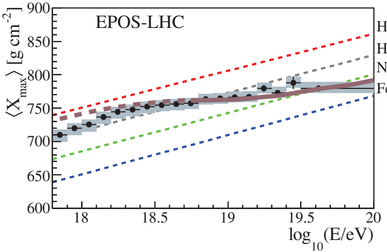

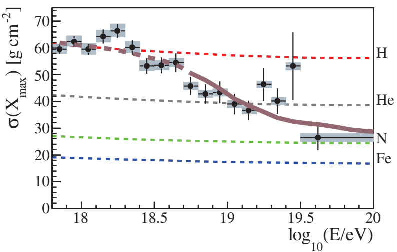

Model describing ankle and mass composition

Unger et al., PRD 92 (2015) 123001

Photo-disintegration in region surrounding acceleration site

High-pass filter: high energy nuclei escape, interactions at low energies produce lighter nuclei with softer spectrum

Injecting silicon with $E_{\max} = Z \times 10^{18.5} = 4.6 \times 10^{19}$ eV, $\gamma = -1$ one gets ankle and complex composition evolution

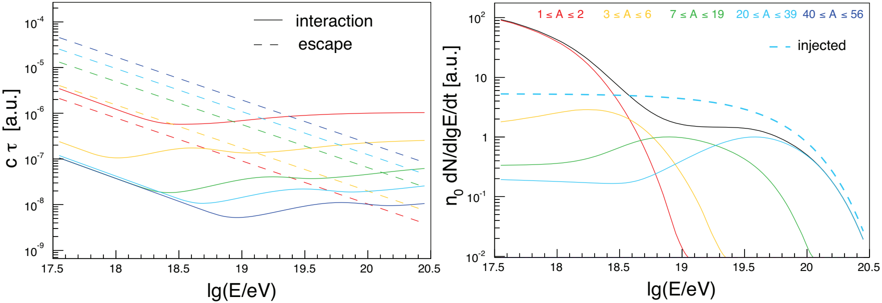

Model describing ankle and mass composition

Unger et al., PRD 92 (2015) 123001

Photo-disintegration in region surrounding acceleration site

High-pass filter: high energy nuclei escape, interactions at low energies produce lighter nuclei with softer spectrum

Injecting silicon with $E_{\max} = Z \times 10^{18.5} = 4.6 \times 10^{19}$ eV, $\gamma = -1$ one gets ankle and complex composition evolution

Good description of Auger data

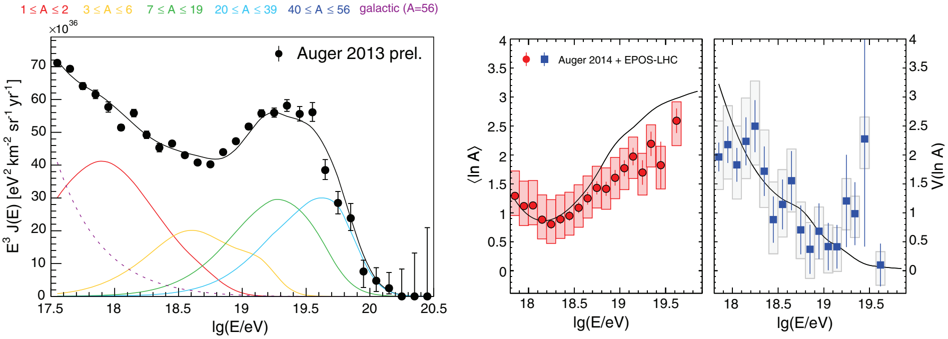

Observation of large-scale anisotropy for $E \geq 8$ EeV

physicsworld TOP 10 BREAKTHROUGH 2017

Science 57 (2017) 1266

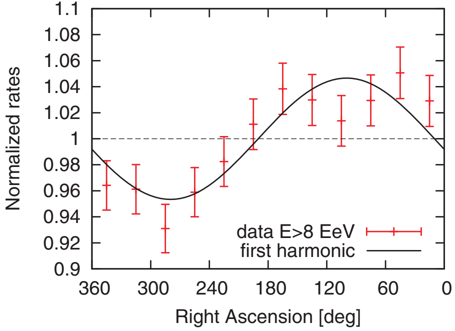

Data set, 1/1/2004–31/08/2016

$0^\circ \leq \theta \leq 80^\circ$

declination $-90^\circ \leq \delta \leq 45^\circ$

85% sky coverage

exposure 76,800 km^2 sr year

Rayleigh analysis in right ascension

Energy (EeV)	Number of events	Amplitude r_α	Phase φ_α (°)	Probability $P(\geq r_\alpha)$
4 to 8	81,701	$0.005^{+0.006}_{-0.002}$	80 ± 60	0.60
≥8	32,187	$0.047^{+0.008}_{-0.007}$	100 ± 10	2.6×10^{-8}

Amplitude for $E \geq 8$ EeV: two-sided Gaussian significance 5.6σ

Observation of large-scale anisotropy for $E \geq 8$ EeV

Science 57 (2017) 1266

Consistency with isotropy for $4~\mathrm{EeV} < E < 8~\mathrm{EeV}$ disfavors dominant galactic CR origin

Energies above 8 EeV

Distance of 125° in dipole direction vs galactic center: better explained by extragalactic CR origin

NB: for $E > 40$ EeV no anisotropies found in direction of galactic center or galactic plane [ApJ 804, 15 (2015)]

Comparing to dipole of 2MASS Redshift Survey catalog of galaxies $(l, b) = (251^\circ, 38^\circ)$

galactic magnetic fields change position of 2MRS dipole (as indicated for $E/Z = 2$ EeV or 5 EeV) and reduce its amplitude (might explain lower amplitude for $4~\mathrm{EeV} < E < 8~\mathrm{EeV}$)

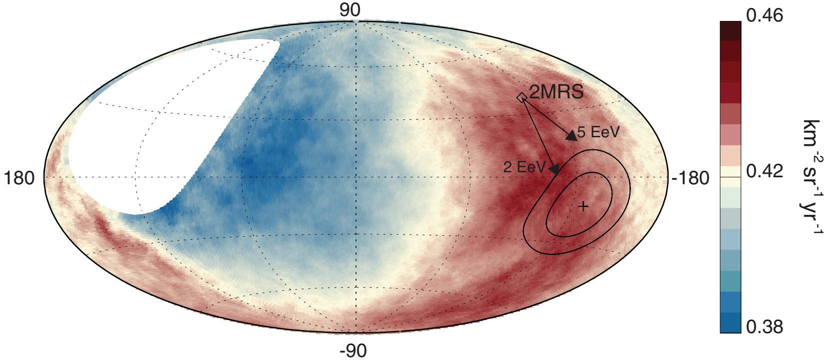

galactic coordinates, Galactic center is at the origin, measured dipole direction is marked with a cross

Correlation with starburst galaxies and γAGNs

ApJL 853 (2018) L29

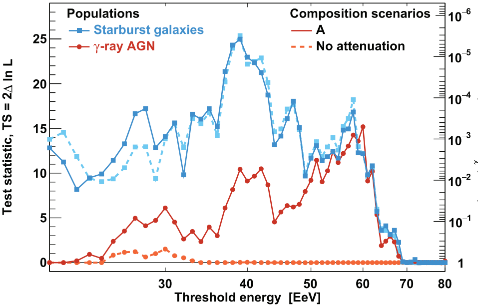

Starburst galaxies

Significance 4σ, $E > 39$ EeV (894 events)

γAGNs

Significance 2.7σ, $E > 60$ EeV (177 events)

starburst galaxies

Observed Excess Map - E > 39 Eev

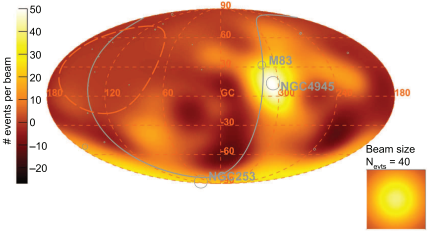

γAGNs

Observed Excess Map - E > 60 Eev

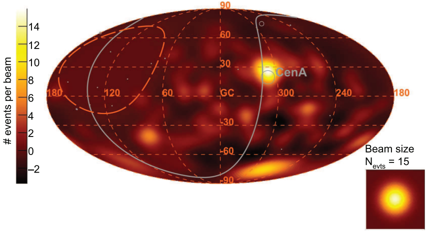

Particle astronomy for mixed composition?

Backtracking (circles — initial directions) using different models of galactic magnetic fields

M. Unger, G. Farrar, ICRC 2017, UHECR 2018

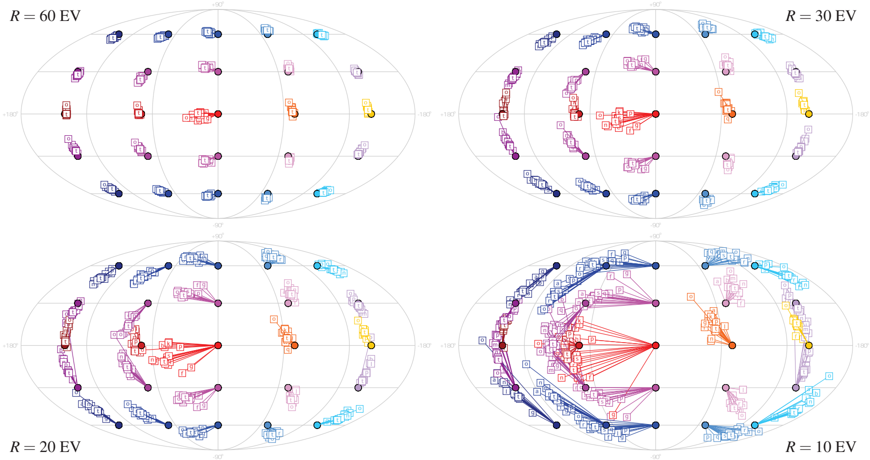

Select low-Z component (if any)

Correct deflections? Restrict analysis to certain sky regions?

Next 10 years: AugerPrime upgrade

International agreement for operation of the Auger Observatory until 2025

Main upgrade

plastic scintillator detectors and radio antennas on all water-Cherenkov stations:
to achieve separation of electromagnetic and muonic components

Aims

Composition sensitivity in the flux suppression region

Sensitivity to 10% proton fraction in this region
(important for GZK photon and neutrino fluxes)

Composition enhanced anisotropy studies

Search for new phenomena in hadronic interactions

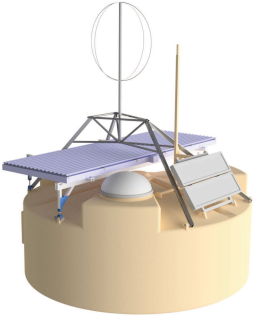

Additional enhancements

FD: increase duty cycle operating in higher night sky background

Underground muon detectors on area of 23.5 km^2

Electronics: sampling rate 120 MHz (currently 40 MHz)
additional small PMTs to increase dynamic range

R. Engel for Auger Collab., ICRC 2015, PoS 686 backups

$\langle X_{max} \rangle$ from Auger and Telescope Array

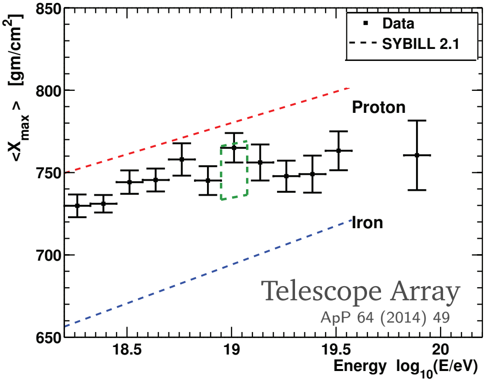

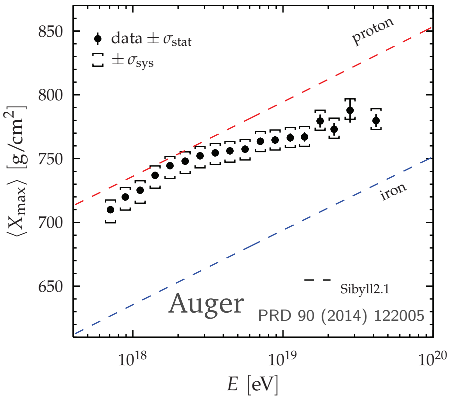

M. Unger for Auger and Telescope Array Collabs., ICRC 2015, PoS 307

$\langle X_{max} \rangle$: Auger vs different TA measurements

A. Yushkov for Auger and TA, UHECR 2018

Discrepancy Auger – TA (Black Rock Mesa/Long Ridge) is larger and energy-dependent

TA Middle Drum

[ApP 64 (2015) 49]

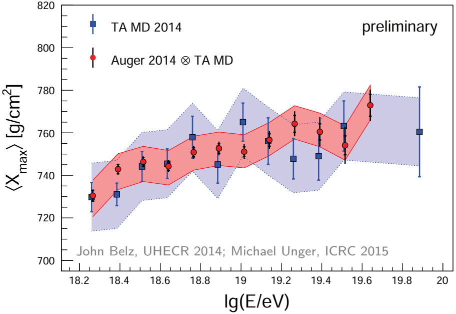

TA Black Rock Mesa/Long Ridge

[ApJ 858 (2018) 76]

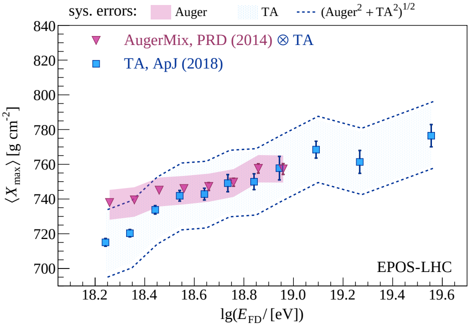

average difference: $\langle \Delta \rangle = (2.9 \pm 2.7\ \text{(stat.)} \pm 18\ \text{(syst.)})\ \text{g/cm}^2$

Auger vs TA

A. Yushkov for Auger and TA, UHECR 2018

$\langle X_{max}^{TA} \rangle < \langle X_{max}^{Auger} \rangle$ for almost all energies

agreement within $(\text{stat} + \text{sys})$ errors

$\sigma(X_{max}^{TA}) > \sigma(X_{max}^{Auger})$ for $\lg(E/\text{eV}) = 18.6 - 19.0$

Next: comparison to Auger ICRC (2017) data and energies $\lg(E/\text{eV}) > 19.0$

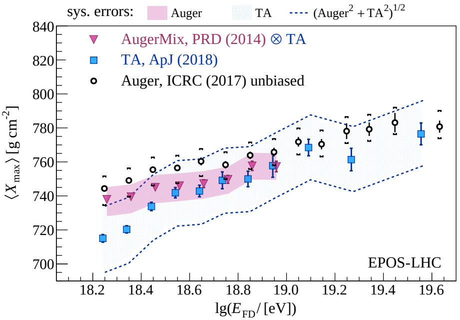

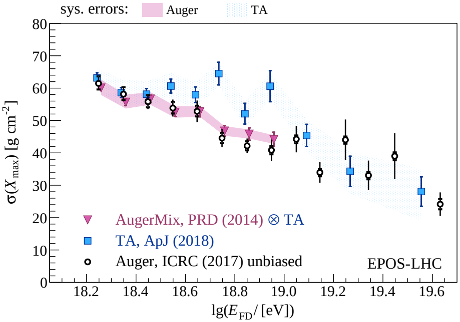

preliminary